


Review

Advancements in Cellular Imaging: Expanding Horizons with Innovative Dyes and Techniques

Payal M. Oak ¹  and Akash S. Mali ^{2,*} ¹ Faculty of Science, Masaryk University, 625 00 Brno, Czech Republic; payal.oak@rediffmail.com² Department of Physiology, Faculty of Science, Charles University in Prague, 128 43 Prague, Czech Republic

* Correspondence: akash.mali@natur.cuni.cz

Abstract: Advancements in cellular imaging have significantly enhanced our understanding of membrane potential and Ca²⁺ dynamics, which are crucial for various cellular processes. Voltage-sensitive dyes (VSDs) are pivotal in this field, enabling non-invasive, high-resolution visualization of electrical activity in cells. This review discusses the various types of VSDs, including electrochromic, Förster Resonance Energy Transfer (FRET)-based, and Photoinduced Electron Transfer (PeT)-based dyes. VSDs are essential tools for studying mitochondrial activity and neuronal function and are frequently used in conjunction with Ca²⁺ indicators to elucidate the complex relationship between membrane potential and Ca²⁺ fluxes. The development of novel dyes with improved photostability and reduced toxicity continues to expand the potential of VSDs in biomedical research. This review underscores the importance of VSDs in advancing our understanding of cellular bioenergetics, signaling, and disease mechanisms.

Keywords: voltage sensitive dyes; mitochondria; Ca²⁺ dynamics; two-photon microscopy; photobleaching

1. Introduction

Cells maintain a crucial biophysical trait known as membrane potential, a fundamental aspect of cellular function. Specialized cells, such as neurons, release chemical neurotransmitters in response to rapid shifts in membrane potential [1]. This potential is generated by the movement of ions like sodium, potassium, and chloride through ion-specific channels in the plasma membrane, following concentration gradients [2]. Electrically excitable cells, including neurons and cardiomyocytes, undergo activation triggered by swift alterations in membrane potential, enduring for hundreds of milliseconds [3]. Conversely, slower fluctuations in resting membrane potential mark various cellular processes such as cell cycle progression, differentiation, insulin secretion, and the circadian firing cycles of SCN neurons [4,5]. To monitor membrane potential changes during specific events, genetically encoded voltage indicators with voltage-dependent fluorescence are commonly employed. Peterka et al. demonstrates that dyes can provide a non-invasive means to observing electrical activity, allowing crucial insights into neuronal function and communication [6].

The three types of VSDs are electrochromic, Förster Resonance Energy Transfer (FRET)-based, and Photoinduced Electron Transfer (PeT)-based dyes, each with distinct mechanisms and applications [3]. Electrochromic VSDs are operated by altering their optical properties in response to variations in the electric field, which lead to rapid and precise detection of membrane potential changes [7]. Gonzalez et al., 1995, revealed that changes in voltage modulate the energy transfer efficiency between two fluorescent molecules in FRET-based VSDs, which results in high sensitivity and specificity [8]. PeT-based VSDs use an electron transfer mechanism to change the fluorescence of the dye, enabling the detection of subtle voltage shifts [9].

VSDs are useful for studying the bioenergetics and dynamics of mitochondria, which are important for both cellular metabolism and apoptosis [10]. Rhodamine 123 and TMRM

**Citation:** Oak, P.M.; Mali, A.S.Advancements in Cellular Imaging: Expanding Horizons with Innovative Dyes and Techniques. *Colorants* **2024**, *3*, 360–377. <https://doi.org/10.3390/colorants3040025>

Academic Editor: Anthony Harriman

Received: 23 July 2024

Revised: 22 November 2024

Accepted: 19 December 2024

Published: 23 December 2024



Copyright: © 2024 by the authors. Licensee MDPI, Basel, Switzerland. This article is an open access article distributed under the terms and conditions of the Creative Commons Attribution (CC BY) license (<https://creativecommons.org/licenses/by/4.0/>).

are commonly used to measure mitochondrial membrane potential, which provides insights into mitochondrial health and function [11]. The relationship between VSDs and calcium (Ca^{2+}) dynamics is another important field of study. VSDs are frequently used with Ca^{2+} indicators to explore the intricate link between membrane potential and intracellular Ca^{2+} levels, which are important for numerous cellular processes, including muscle contraction and neurotransmitter release [12]. Fluo-4 and Fura-2 dyes are frequently used in Ca^{2+} imaging, providing high-resolution temporal and spatial data on Ca^{2+} dynamics [13]. Two-photon microscopy, linked with VSDs, has altered the capacity for electrical activity in deep tissue sections with low photodamage and high spatial resolution [14].

Common challenges related to the application of VSDs include photobleaching, where constant exposure to light decreases dye fluorescence, and autofluorescence, which can interfere with signal detection [15]. Recent advancements include the development of new dyes with enhanced sensitivity, better photostability, and reduced toxicity, expanding the potential of VSDs in various fields [16].

2. Types of Voltage Sensitive Dyes

Voltage-sensitive dyes (VSDs) are applied to the cell membrane externally and change their optical properties with transmembrane potential, providing direct measurements of neuronal activity at sub-millisecond temporal resolution. In combination with high-magnification microscopy, VSD can image neuronal activity in single cells. Confocal and two-photon technology can further increase the effective spatial resolution [17]. The basic principle is to employ voltage-sensitive dyes to transform the change in membrane potential into a fluorescent signal, and then detect the change in fluorescence signal intensity to reflect the change in the electrical signal [18]. Previous reports discovered that, after opening the skull and the dura mater of the animal, the dye molecules are applied on the surface of the cortex [19]. They bind to the external surface of the membranes of all cells without interrupting their normal function and act as molecular transducers that transform changes in membrane potential into optical signals. More precisely, once excited with the appropriate wavelength, VSDs emit instantaneously an amount of fluorescent light that changes membrane potential, thus allowing for an excellent temporal resolution for neuronal activity imaging. The fluorescent signal is proportional to the membrane area of all stained elements under each measuring pixel. Voltage-sensitive dyes are fluorescent molecules capable of detecting changes in membrane potential. The next generation of direct dyes, which exhibit enhanced sensitivities and temporal resolutions due to molecular electronic changes, can be classified into three types: (i) Electrochromic dyes, (ii) Förster resonance energy transfer (FRET)-based dyes, and (iii) Photoinduced electron transfer (PeT)-based dyes [19].

(A) Electrochromic Dyes:

Electrochromic dyes, often referred to as 'fast' dyes, present an optimal solution for detecting swift neuronal voltage fluctuations owing to their rapid response rate [20]. In the electronic ground state, the chromophore's asymmetry results in an asymmetric electron system, with delocalized electrons at the anilino group, and the pyridyl group at the center bearing a positive charge [21]. When a molecule binds to a membrane, the positively charged pyridine ring is positioned near the extracellular space, with its long axis perpendicular to the membrane surface [22]. Upon photoexcitation, the positive charge center undergoes movement during the absorption process from pyridine to aniline and reverses during the emission process back to pyridine. The energy required for excitation and emission fluctuates in the presence of charge transfer in an external electric field, depending on whether the process occurs parallel to or perpendicular to the electric field direction. Electrochromic dyes offer the advantage of ultrafast fluorescence response to voltage alterations, enabling researchers to observe processes with sub-millisecond temporal resolution (Figure 1).

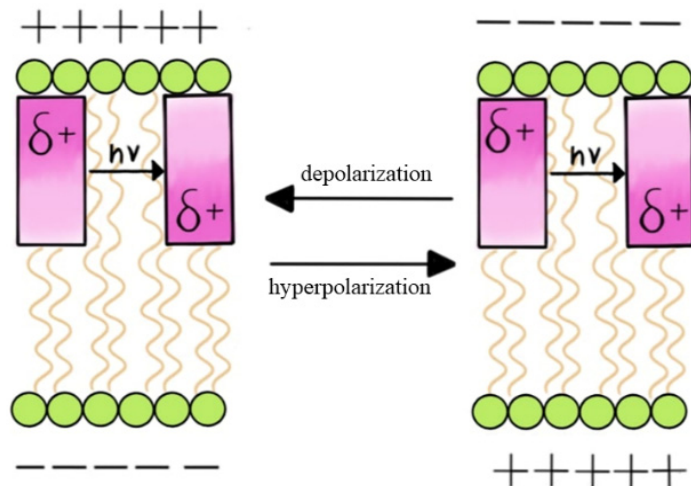


Figure 1. Electrochromic dyes respond to voltage through a direct interaction between the chromophore and the electric field [23].

(B) Förster Resonance Energy Transfer (FRET)-based Dyes

FRET fluorescent sensors contain both a donor and an acceptor, and those are fluorescent chromophores [24]. When these chromophores are positioned within an optimal distance from each other, typically between 2 and 10 nanometers, non-radiative energy transfer occurs, resulting in a reduction in donor fluorescence intensity and an enhancement in acceptor fluorescence intensity [25]. FRET technique enables the detection of various biological phenomena such as protein–protein interactions, structural changes in proteins, and the activity of signaling proteins like protein kinases and small GTPase [26,27]. FRET biosensors commonly employ three main types of fluorophores: small organic dyes, fluorescent proteins (FPs), and quantum dots (QDs) [24]. Additionally, to ensure adequate energy coupling between the two molecules, there must be spectral overlap between the emission spectrum of the donor and the excitation spectrum of the acceptor, constituting the second fundamental requirement for FRET [28]. A minimum overlap of 30% is necessary to facilitate sufficient FRET for accurate detection [29]. When these dyes are incorporated into the cell membrane, changes in membrane potential can alter the conformation of the dye molecules, affecting the distance between the donor and acceptor. This results in voltage-dependent changes in FRET efficiency, which can be measured as changes in fluorescence [30] (Figure 2).

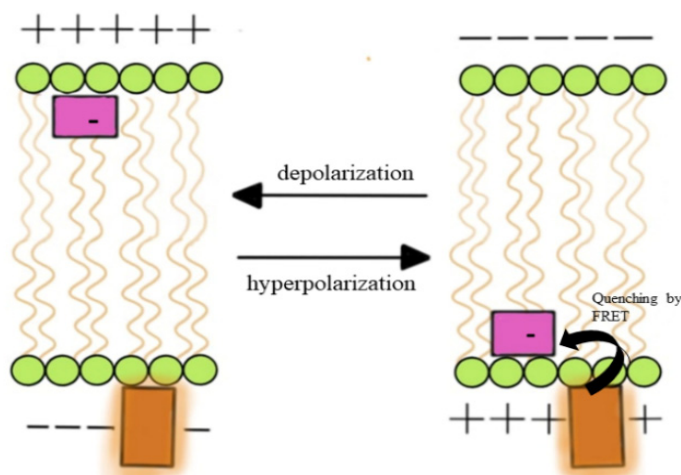


Figure 2. FRET-based voltage sensors use lipophilic anions that intercalate into the cellular membrane and distribute between the inner and outer leaflets depending upon the transmembrane potential [23].

(C) Photoinduced Electron Transfer (PeT)-based Dyes

Fluorescent probes often utilize photoinduced electron transfer (PeT), a classical electron transfer method [31]. In 1985, De Silva generalized the application of PeT in the creation of systems based on molecular logic gates and fluorescence sensors [32]. Due to their high signal-to-noise ratios, PeT-based fluorescent probes have maintained significant interest among chemical, biological, and medical researchers for over 40 years [33]. Common PeT-based fluorescent probes are multi-component systems where an unconjugated linker connects a fluorophore to an activating or recognition group [34]. These probes are highly effective for cellular imaging and disease diagnosis due to their strong fluorescence amplification towards the target and minimal fluorescence background. PeT dyes are widely used for tracking cellular processes, visualizing protein localization, and studying protein–protein interactions within cells [35].

PET-based VSDs show that the membrane potential affects the rate of electron transfer between a donor and an acceptor within the dye molecule [36]. In these dyes, the donor and acceptor are positioned such that electron transfer can occur when the molecule is excited by light [37]. The efficiency of this electron transfer process is modulated by the membrane potential, which in turn alters the fluorescence intensity of the dye. This mechanism allows for the detection of voltage changes through changes in fluorescence, providing a direct optical readout of membrane potential dynamics [21] (Figure 3).

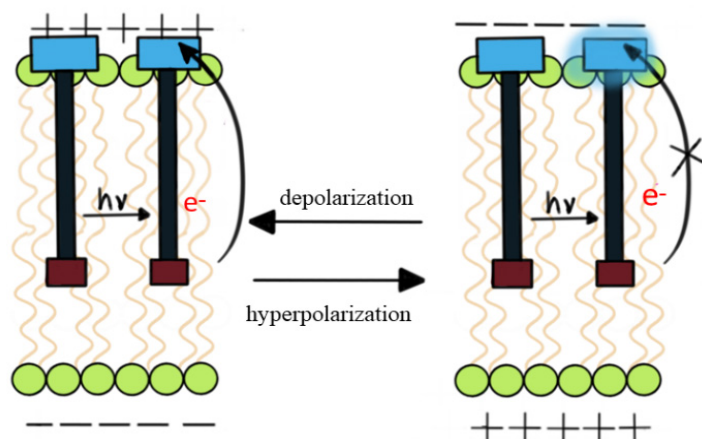


Figure 3. Molecular wire PeT VSDs depend upon the voltage-sensitive electron transfer from an electron-rich donor through a membrane-spanning molecular wire to a fluorescent reporter [23].

3. Mitochondrial Activity and Voltage-Sensitive Dyes

Adenosine triphosphate (ATP) is generated in the mitochondria through oxidative phosphorylation, and this process is linked with electron transport chain (ETC), which is why mitochondria are known as the powerhouse of cells [38]. Mitochondria play an important role in reactive oxygen species (ROS) signaling, calcium homeostasis, and the intrinsic pathway of apoptosis [39]. The mechanism of mitochondrial function depends on the ETC, which produces proton gradients across the inner mitochondrial membrane [40]. Mitochondrial membrane potential ($\Delta\psi_m$), also known as an electrochemical gradient, drives ATP synthesis via ATP synthase [41]. Various diseases such as cancer, neurodegenerative diseases, and metabolic disorders are associated with disruptions in mitochondrial function [42,43]. Mitochondria serve as hubs for cellular signaling and metabolic integration [44].

VSDs are used to detect processes in living cells and give information about the activity of mitochondria. VSDs alter their fluorescence intensity to respond to changes in membrane potential [45]. High sensitivity to voltage changes, excellent spatial resolution, and rapid temporal resolution are key characteristics of VSDs [46]. In the mechanism of voltage sensitive dyes, dye molecules will be redistributed within a membrane in response to voltage changes, which results in alteration in their fluorescence properties. VSDs allow

real-time monitoring of cellular events without disturbing cell functions due to their non-invasive nature [47]. In VSDs, the electron transfer mechanism includes multiple complex phases. Initially dye molecules are integrated into the membrane of the mitochondria, where they sense the electric field that crosses the membrane [41]. VSD molecules transform into an excited state in light and become highly sensitive to the local electric field [48].

Zorova et al., 2018, points out the significance of the mitochondrial electron transport chain (ETC) activity in altering VSD fluorescence [41]. The ETC develops a proton gradient resulting in a significant membrane potential across the inner mitochondrial membrane, detectable by VSDs, providing insights on ETC activity and overall mitochondrial health. Genetic mutations or mitochondrial toxins can create disruptions in the ETC, which can lead to alterations in VSD signals and a drop in membrane potential [49]. A study revealed that the chemical targeting of VSDs to specific cells increases their use in live-cell imaging [50]. To address photostability-related concerns, Hernández-Juárez et al., 2021, developed a fluorescent probe that can dynamically assess mitochondrial membrane potential [51]. Refer to Table 1 for an overview of voltage-sensitive dyes used in mitochondrial research.

Table 1. Voltage-sensitive dyes for mitochondrial studies.

	Voltage Sensitive Dyes	Uses	Drawbacks	Advantages	References
1.	JC-1	Accumulates in mitochondria, exhibits red fluorescence. Fluoresces green and monomeric in depolarized mitochondria.	Aggregation-dependent fluorescence can lead to quenching and sensitivity to experimental condition.	Due to the color change, it differentiates healthy and depolarized mitochondria.	Sivandzade et al., 2019 [52]. Perry S.W. et al., 2011 [53]
2.	Rhodamine 123	Used to observe mitochondrial membrane potential. Aggregates in mitochondria in a potential-dependent manner.	Over time due to photobleaching, rhodamine 123 lost its fluorescence.	It is specific for mitochondrial potential.	Baracca et al., 2003 [54]. Zorova et al., 2018 [41]
3.	Di-8-ANEPPS	Primarily used for plasma membrane potential but can be adapted for mitochondrial studies due to its sensitivity to voltage change.	Its fluorescence is affected by changes in the membrane potential.	Highly sensitive to voltage changes.	Carlo Manno et al., 2013 [55] Youngworth et al., 2023 [56]
4.	TMRM (Tetramethyl-rhodamine methyl ester)	It provides precise measurements of mitochondrial membrane potential.	To avoid toxic effects at high concentration it requires careful optimization.	Potential dependent dye.	Ernst et al., 2023 [57], Creed et al., 2019 [58].
5.	MitoTracker Red CMXRos	Exhibits red fluorescence in active mitochondria; convenient for live-cell imaging of mitochondrial potential and dynamics.	It affects mitochondrial function. It binds to mitochondrial proteins and lipids; not dependent on mitochondrial potential.	Precise for live-cell imaging.	Kholmukhamedov et al., 2013 [59]. Buravkov S.V. et al., 2014 [60] Neikirk et al., 2023 [61]

Table 1. Cont.

Voltage Sensitive Dyes	Uses	Drawbacks	Advantages	References
6. MitoSOX Red	Analyses superoxide production in mitochondria, indicating mitochondrial oxidative stress by fluorescing upon oxidation.	It becomes super oxidized and affects mitochondrial functions.	It is specific for detection of mitochondrial oxidative stress.	Wang Q et al., 2018 [62], Roelofs et al., 2015 [63] Mali et al., 2023 [42].
7. Safranin O	Accumulates in mitochondria in a potential-dependent manner; used for dual or multi-parameter assessments of mitochondrial function.	Under high-dye concentration, fluorescence can be quenched.	Useful in multi-parameter assessments of mitochondrial functions.	Krumshnabel et al., 2014 [64], Chowdhury et al., 2016 [65].
8. JC-10	Improved version of JC-1 with better solubility; used for similar applications to monitor mitochondrial membrane potential changes.	It has a higher cost compared to JC-1.	It has better solubility.	Nadin et al., 2022 [66], Sakamuru et al., 2017 [67].
9. DASPMI (4-(4-Diethylaminostyryl)-N-methylpyridinium iodide)	Stains active mitochondria and measures mitochondrial membrane potential with high sensitivity.	It is less compatible with live-cell imaging.	Highly sensitive for active mitochondria.	Ramadaas et al., 2008 [68].

4. Voltage Sensitive Dyes and Ca²⁺ Dynamics

Voltage-sensitive dyes indirectly determine Ca²⁺ fluxes by identifying changes in membrane potential [69,70]. Oh et al., 2015, discovered the use of VSDs in combination with Ca²⁺ imaging to observe Ca²⁺ fluxes in neuronal tissue, providing insights into synaptic activity and plasticity [71]. Similarly, VSDs in brain slices examine neuronal circuit dynamics, capturing rapid changes in membrane potential that are important to understanding the temporal characteristics of Ca²⁺ signaling [41,72]. The use of VSDs in conjunction with Ca²⁺ imaging for studying dendritic functions in living animals was revealed by Grienberger et al., 2015 [73]. They emphasized the vital role of membrane potential alteration in shaping Ca²⁺ dynamics within dendrites. Scientist studied the application of optogenetics coupled with VSDs for multicolor control and imaging of neuronal activity, enabling for precise control and monitoring of Ca²⁺ dynamics [74]. A method for all-optical electrophysiology was presented by Hochbaum et al., 2014, using VSDs to assess change in membrane potential in response to optogenetic stimulation, offering an effective way of studying Ca²⁺ dynamics in response to controlled electrical activity [75]. A novel approach for evolving fluorescent voltage reporters with enhanced properties, offers greater sensitivity and dynamic range for better visualization of membrane potential and associated Ca²⁺ fluxes [76].

Aseyev et al., 2023, recorded fast neuronal activity with the help of voltage imaging, showing the development of potentiometric probes for simultaneous recording of multiple neurons [72]. Djemai M et al. (2023) assessed intracellular Ca²⁺ fluctuations and changes in membrane potential in cardiomyocytes produced from induced pluripotent stem cells using optical mapping. Fisher et al., 2008, revealed the advantages of two-photon excitation

of fluorescent VSDs for monitoring membrane potential changes in mammalian nerve terminals in situ. These studies highlight the importance of VSDs in understanding the intricate relationship between membrane potential and Ca^{2+} dynamics, leading to a better understanding of cellular signaling and function [7,77,78]. Refer to Table 2 for an overview of voltage-sensitive dyes used in Ca^{2+} imaging.

Table 2. Voltage-sensitive dyes for Ca^{2+} imaging.

Voltage Sensitive Dyes	Uses in Ca^{2+}	Drawbacks	Advantages	References
1. Fura-2	A ratiometric dye that binds to Ca^{2+} and exhibits a shift in its fluorescence excitation spectrum, allowing for quantitative measurements of intracellular Ca^{2+} concentrations.	Fura-2 requires UV excitation, and it has increasing risk of phototoxicity.	Accurate ratiometric measurements of Ca^{2+} levels.	Patricia Santofimia-castano et al., 2016, Tanka et al., 2021 [79,80]. Li ES. et al., 2021 [81]
2. Fluo-4	Fluo-4 increases fluorescence intensity upon binding to Ca^{2+} ; it is a non-ratiometric dye. Used for imaging rapid Ca^{2+} transients.	It's non-ratiometric nature can lead to signal distortions caused by dye concentration and photo bleaching.	High sensitivity to fast Ca^{2+} transients.	Schneidereit D et al., 2016, Gee et al., 2000 [82,83] Pydi, S.P. et al., 2014 [84]
3. GCaMPs	Genetically encoded calcium indicators that combine a fluorescent protein with a Ca^{2+} binding domain.	Compared to synthetic dyes, GCaMPs have a slower response time.	High specificity and sensitivity.	Shen et al., 2018 Berlin et al., 2015 [85,86] Cho, J. et al., 2017 [87]
4. Rhod-2	This dye is particularly useful for studying mitochondrial Ca^{2+} dynamics and it has a red fluorescence.	Cytotoxicity risk is higher.	Due to its red fluorescence, effective imaging of mitochondrial Ca^{2+} levels.	Drummond et al., 2000 [88] Gryniewicz et al., 1985 [89]
5. Cal-590	A red-emitting dye that is useful for multiplex imaging with green and blue fluorophores, providing bright fluorescence.	Limited commercially available data on biological compatibility.	High signal-to-noise ratio.	Tischbirek et al., 2015 [90]
6. Cal-520	It is suitable for high-throughput screening and imaging applications.	It is sensitive to loading variability and photobleaching like other non-ratiometric dyes.	A green, fluorescent dye with improved brightness and signal-to-noise ratio compared to Fluo-4.	Lock et al., 2015 [91]
7. Oregon Green 488 BAPTA-1 (OGB-1)	Used for detecting rapid Ca^{2+} changes in neuronal and other excitable cells.	Non-ratiometric nature may show some errors in heterogeneous tissue environment.	A highly sensitive dye with fast kinetics.	Russell et al., 2011, Tada et al., 2014 [13,92]
8. Indo-1	A ratiometric dye that allows reducing artifacts caused by dye concentration or cell thickness variations.	Indo-1 requires UV excitation, increasing phototoxicity risk.	Dual-emission measurements, providing accurate quantification of Ca^{2+} levels.	Bannwarth et al., 2009 [93] Ryan, J. et al., 2011 [94]

5. Voltage-Sensitive Dyes and Two-Photon Microscopy

Two-photon microscopy and voltage-sensitive dyes are an effective combination for developing live-cell imaging methods, offering an in-depth understanding of cellular and neuronal processes. VSDs are important for measuring membrane potential changes and for directly observing electrical activity in excitable cells like heart and neuronal tissues [95]. This capability allows for a comprehensive analysis of neuronal circuits and the study of electrophysiological phenomena with high spatial and temporal resolution [96]. When compared to conventional one-photon excitation, two-photon microscopy provides a complementary method because it uses near-infrared light for excitation, which reduces phototoxicity and photobleaching [97]. This technique is beneficial for imaging thick tissues and living organisms as it allows for deeper tissue penetration and reduces out-of-focus light, thus providing clearer and more detailed images. Homma et al., 2009, observed that the combination of VSDs and two-photon microscopy improves the ability to monitor dynamic processes within intact tissues, such as brain slices or even whole animals, with minimum photodamage [98].

This dual approach is strengthened by the intrinsic benefits of two-photon excitation, such as the ability to excite fluorescent dyes with lower energy photons, resulting in less phototoxicity and greater tissue penetration. This ability is important for imaging highly scattering tissues, such as in the brain where high levels of light absorption and scattering can make it difficult to obtain clear images with one-photon microscopy [99]. Researchers can obtain higher depth resolution and lower background noise by using two-photon microscopy, which makes it possible to conduct accurate studies of cellular dynamics in their natural environment [100]. VSDs with two-photon microscopy have proven valuable tools for neuroscience research, particularly in the study of synaptic activities and network dynamics [101]. This combination allows for simultaneous imaging of electrical activity across multiple neurons, providing insights into how neuronal circuits process information. Additionally, the ability to image *in vivo* with minimal invasiveness has opened new avenues for studying the development and function of neuronal networks in live animals, leading to a deeper understanding of brain function and dysfunction [102].

6. Common Issue and Solutions During Imaging

6.1. Photobleaching

When fluorescent dyes lose their capacity to emit light due to prolonged exposure to excitation, light can lead to a reduction in signal intensity over time, compromising the data quality, which causes photobleaching. To reduce photobleaching, researchers frequently use anti-fade reagents that protect the fluorophores from oxidative damage [103]. Using time-lapse imaging and optimizing laser setting can reduce light exposure intensity and duration, preserving fluorescence signal [104]. Using fluorophores with intense photostability is another effective strategy [105].

6.2. Autofluorescence

When a specific wavelength induces autofluorescence, biological structures emit light naturally. This background signal may cover the fluorescence of labeled probes, resulting in decreased sensitivity and specificity in imaging. Researchers frequently use spectral unmixing techniques, which separate the background autofluorescence from the fluorescence signals of interest depending on their spectral properties, to address autofluorescence. Using near-infrared dyes is an alternative approach; these dyes usually experience less autofluorescence interference because of the weaker background signals in their spectral region [106]. Chemical treatments that quench autofluorescence, like Sudan black B or sodium borohydride, can also be effective [107].

7. Dyes and Their Application in Neuroscience and Cell Biology

Voltage-sensitive dyes (VSDs) are used in the detection and imaging of electrical activity across biological membranes, diverse applications in neuroscience, cardiology, and cell biology. Among them, ArcLight has a tendency to observe single action potentials and sub-threshold events in neurons, providing critical insights into cellular electrophysiology [108]. QuasAr allows all-optical electrophysiology in mammalian neurons, integrating voltage imaging with optogenetic control for advanced neural circuit studies [75]. Ace2N-mNeon is useful for high-speed recording of neural spikes in awake animals, enabling the real-time investigation of brain activity [109]. Voltron offers unparalleled stability and reliability for long-term in vivo voltage imaging [110]. Flare's dual-color emission capability improves its versatility through allowing the simultaneous imaging of voltage changes and other cellular processes [111]. Near-infrared (NIR) dyes are particularly useful for imaging in live and intact organisms due to their deep tissue penetration and reduced phototoxicity [112]. ANNINE demonstrates high sensitivity and rapid response, making it ideal for capturing fast electrical events [87], while Di-4-ANEPPS and Di-8-ANEPPS are frequently used for membrane potential imaging in cardiac and neural tissues, offering precise visualization of dynamic processes [50,113,114]. Rhodamine, important for its brightness and stability, is employed across various imaging applications, showcasing the breadth of voltage-sensitive dye utility in modern biological research [115].

8. Synthesis of ANNINE and Chromene-Based VSDs

Hubener et al., 2003, developed the ANNINE dyes by combining four different donor moieties (D1–D4) and two different acceptor moieties (A1–A2) [116]. Four steps were involved in the synthesis of Triphenylphosphonium salt D1 from 3-aminobenzoic acid, 3-N,N-dibutylaminobenzyl alcohol (LiAlH₄), 3-N,N-dibutylaminobutyl benzoate (1-iodobutane and K₂CO₃) [117], 3-N,N-butylaminobenzyl chloride (with PCl₅), and lastly treatment with PPh₃. This method improves the synthesis using 3-aminobenzaldehyde dimethyl acetal as a starting material [118]. Hubener et al. brominated 2-nitronaphthalene to synthesize 1-bromo-6-nitronaphthalene [116] that was subsequently reduced to 6-amino-1-bromonaphthalene (SnCl₂, HCl) in order to synthesize D2. When 1-iodobutane was alkylated it led to the formation of 1-bromo-6-N,N-dibutylaminonaphthalene. 6-N,N-dibutylaminonaphthalene-1-carboxylic acid (NaOH) and 6-N,N-dibutylamino-1-cyanonaphthalene (CuCN) are produced by reducing 6-N,N-dibutylamino-1-hydroxymethylnaphthalene with LiAlH₄ (a direct synthesis starting from 1-bromo to 6-N,N-dibutylaminonaphthalene via the lithiated intermediate and subsequent reaction with formaldehyde was less effective). After the bromination (PBr₃) of the alcohol, treatment with PPh₃ resulted in D2. A Wittig reaction was carried out to combine D1 with 2-methoxymethylbenzaldehyde to form D3 [119]. Photocyclization of the alkenes E/ZZ-(3-N,N-dibutylaminostyryl)benzylmethyl ether yielded 7-N,N-dibutylamino-1-methoxymethylphenanthrene. 7-N,N-dibutylamino-1-bromomethylphenanthrene was synthesized through ether cleavage, and it was combined with triphenylphosphine to produce D3. Starting with D2, the same reaction sequence was used to obtain D4 (Figures 4 and 5).

A previous study employed a less straightforward approach to work around the unstable aminochromene (3–6). Cu(I)-catalyzed [2+2] cycloaddition of o-formylaryl propargyl ether 4 in the presence of malononitrile is the first step that produces the deeply colored push–pull chromophore 5 [120]; in the presence of water, NaOH hydrolyses this to aldehyde 6. Pyrrolidine was used as a catalyst to condense the resulting aldehyde with either fluorinated pyridinium 7 or fluorinated quinolinium 8 to provide the desired hemicyanine colors [59]. To achieve a good balance between dye solubility and delivery in the aqueous medium vs. persistent membrane staining for cells and biological tissues, three distinct alkyl groups *n*-butyl, *n*-pentyl, and *n*-hexyl have been incorporated as lipid membrane anchors. Compared to their isostructural amino-chromene dyes, they tend to be more water soluble and less persistent on cells and tissues; however, this issue was readily solved by using the dipentyl or dihexyl VSDs (Figure 6).

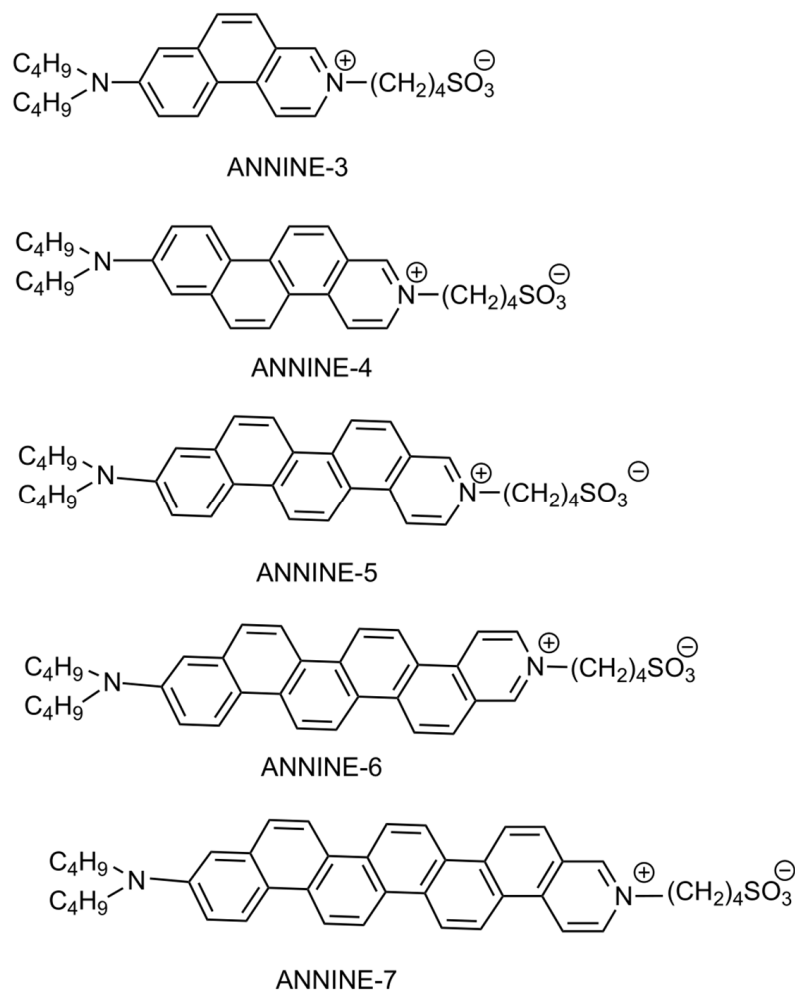


Figure 4. Chemical structure of ANNINE. Reproduced with permission from [116], 2003, ACS.

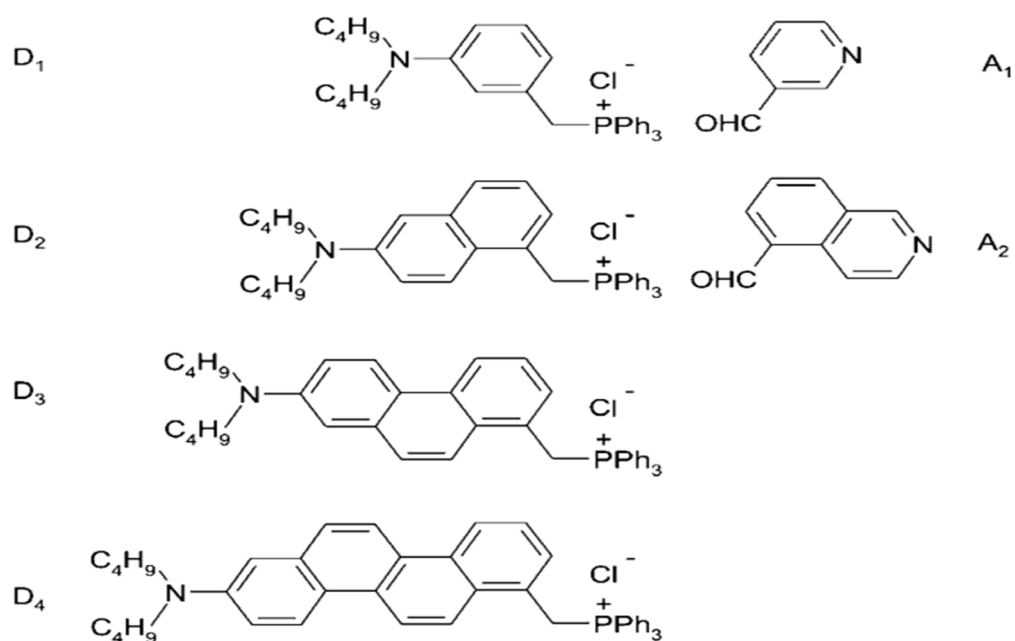


Figure 5. Synthesis of the ANNINE dyes. Reproduced with permission from [116], 2003, ACS.

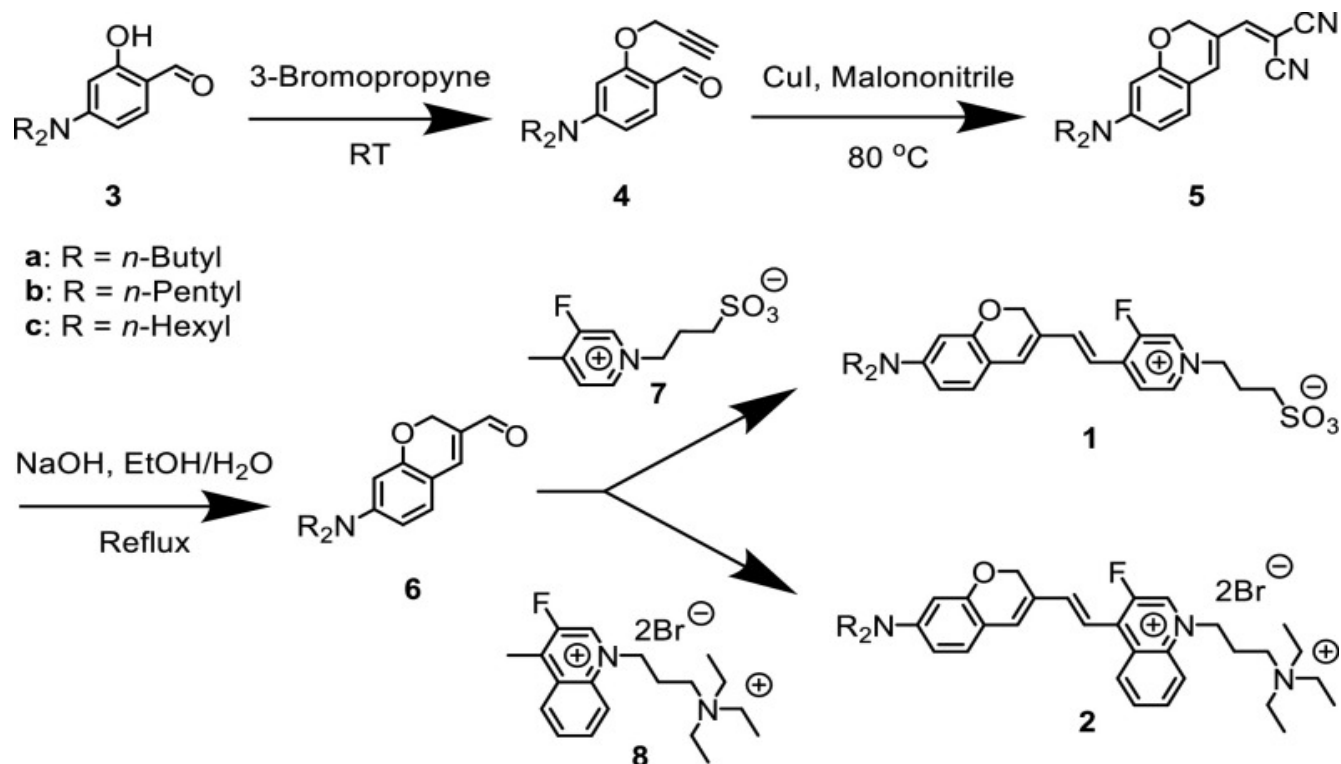


Figure 6. Synthesis of chromene-based VSD [44].

9. Recent Advances in Voltage-Sensitive Dyes

9.1. Enhancements in Sensitivity and Specificity

Recent developments in VSDs have focused on increasing their sensitivity and specificity to better capture rapid changes in membrane potential. A significant development is the release of ANNINE-6plus, a better dye that provides stronger membrane binding and greater water solubility than ANNINE-6 dye [121]. Due to its high voltage sensitivity, this dye can be used for high-resolution imaging of neuronal activity [122]. VSDs like QuasAr and Archon1 have been designed to supply higher signal-to-noise ratios along with faster reaction times, allowing action potential monitoring in real-time with unprecedented accuracy [123].

9.2. Expansion of Spectral Range

The expansion of the spectral range of VSDs is another significant development. Spectral congestion is a common issue with traditional VSDs when used in combination with other fluorescent markers [124]. Researchers have developed novel VSDs that work at different wavelengths to overcome spectral congestion, i.e., blue-shifted variants like CheRiff were improved to increase their compatibility with optogenetic tools, permitting simultaneous optical stimulation and voltage imaging without spectral overlap [125–127]. ReaChR and ChRmine are examples of red-shifted dyes that allow deeper tissue penetration and minimize interference with commonly used blue light-activated optogenetic proteins [128].

9.3. Genetically Encoded Voltage Indicators (GEVIs)

Voltage imaging has experienced a paradigm shift with the development of genetically encoded voltage indicators (GEVIs) that overcome some of the drawbacks of conventional synthetic dyes by providing cell-type specificity and long-term expression in living [129]. Advanced GEVIs, such as ASAP3 and Voltron, have the ability to react rapidly and reverse voltage change, allowing the continuous observation of neuronal dynamics in vivo. These tools have created new opportunities for studying complex brain functions and network activities with high temporal and spatial resolution [130].

9.4. Applications in Cardiac Research

VSDs are making significant contributions to cardiac research [131]. In order to better understand arrhythmias and how electrical impulses flow through heart tissue, optical mapping techniques using VSDs have become important. Recent studies have utilized advanced VSDs to achieve high-resolution mapping of action potentials and Ca^{2+} transients in cardiomyocytes derived from induced pluripotent stem cells (iPSCs), providing insights into the mechanisms underlying cardiac diseases [7].

10. Future Perspectives of Voltage-Sensitive Dyes (VSDs)

Voltage-sensitive dyes (VSDs) have the potential to improve electrophysiology and bioimaging. To detect sub-threshold voltage fluctuations and action potentials accurately, sensitivity and signal-to-noise ratios need to be improved [132,133]. Improving deep-tissue imaging through the development of dyes with near-infrared (NIR) fluorescence is possible for non-invasive and phototoxicity-free in vivo applications [134]. According to Sirbu D et al., it is expected that the combination of VSDs with modern techniques like multiphoton microscopy and optogenetics would allow simultaneous stimulation and imaging of neural networks, expanding their application in neuroscience [135]. These dyes are currently used in areas other than neuroscience, such as cardiology and oncology. For example, monitoring cellular responses or arrhythmias to therapeutic agents is now possible through improved VSD technologies [115]. Future designs also focus on reducing cytotoxicity and improving dye stability for long-term imaging in live tissues, facilitating translational research and potential clinical applications [133].

11. Drawbacks of Chromene-Based and ANNINE Dyes

Chromene-based VSDs are highly recommended for their simple synthesis and high sensitivity. Chromene-based dyes have poor photostability, limiting their effectiveness during prolonged imaging sessions, as photobleaching could reduce signal reliability [6]. They exhibit less effective results at a physiological pH, potentially decreasing sensitivity under biological conditions [136]. Particularly in thick tissues or in vivo imaging contexts, chromene-based dyes have limited ability to cross lipid bilayers efficiently. This limits their labeling efficiency and diffusion [137].

ANNINE dyes are known for their favorable signal-to-noise ratios and brighter fluorescence, but ANNINE dyes have cytotoxic effects at high concentrations, which can limit cell viability during long-term research, and are less appropriate for live-cell imaging [138]. Distorted voltage measurements and nonlinear fluorescence can be caused due to aggregation of ANNINE dyes within lipid bilayers [138]. The emission spectra of ANNINE dye frequently overlaps with other fluorophores, limiting multi-color imaging applications and their ionic strength, sensitivity to temperature, and other environmental factors affect their value across experimental setups [3].

12. Conclusions

Recent developments in voltage-sensitive dyes have significantly increased our understanding of membrane potential dynamics, important for various cellular processes. These dyes, through high-resolution, non-invasive imaging, have become invaluable in fields like neuroscience and cardiac research. Recent advancements in electrochromic, Förster Resonance Energy Transfer (FRET)-based, and Photoinduced Electron Transfer (PeT)-based dyes has expanded their applications, allowing precise detection of membrane potential changes. Challenges such as photobleaching and autofluorescence have been mitigated through advancements in dye chemistry and imaging techniques, including two-photon microscopy, which allows deeper tissue imaging with reduced photodamage. The integration of VSDs with Ca^{2+} imaging has revealed the intricate relationship between membrane potential and Ca^{2+} dynamics. Novel dyes with improved photostability, sensitivity, and reduced toxicity continue to expand VSDs' potential in biomedical research. Thus, VSDs have revolutionized cellular imaging, offering unparalleled temporal and spatial resolution,

driving discoveries in cellular physiology, and aiding the development of diagnostic and therapeutic strategies.

Author Contributions: Conceptualization, P.M.O. and A.S.M.; resources, A.S.M.; data curation, P.M.O. and A.S.M.; writing—original draft preparation, P.M.O.; writing—review and editing, A.S.M.; supervision, A.S.M. All authors have read and agreed to the published version of the manuscript.

Funding: This research received no external funding.

Institutional Review Board Statement: Not applicable.

Informed Consent Statement: Not applicable.

Data Availability Statement: No new data were created or analyzed in this study.

Conflicts of Interest: The authors declare no conflict of interest.

References

1. Liu, P.; Miller, E.W. Electrophysiology, Unplugged: Imaging Membrane Potential with Fluorescent Indicators. *Acc. Chem. Res.* **2020**, *53*, 11–19. [[CrossRef](#)]
2. Bean, B.P. The Action Potential in Mammalian Central Neurons. *Nat. Rev. Neurosci.* **2007**, *8*, 451–465. [[CrossRef](#)] [[PubMed](#)]
3. Nikolaev, D.M.; Mironov, V.N.; Shtyrov, A.A.; Kvashnin, I.D.; Mereshchenko, A.S.; Vasin, A.V.; Panov, M.S.; Ryazantsev, M.N. Fluorescence Imaging of Cell Membrane Potential: From Relative Changes to Absolute Values. *Int. J. Mol. Sci.* **2023**, *24*, 2435. [[CrossRef](#)] [[PubMed](#)]
4. Sundelacruz, S.; Levin, M.; Kaplan, D.L. Membrane Potential Controls Adipogenic and Osteogenic Differentiation of Mesenchymal Stem Cells. *PLoS ONE* **2008**, *3*, e3737. [[CrossRef](#)]
5. Belle, M.D.C.; Diekman, C.O.; Forger, D.B.; Piggins, H.D. Daily Electrical Silencing in the Mammalian Circadian Clock. *Science* **2009**, *326*, 281–284. [[CrossRef](#)] [[PubMed](#)]
6. Peterka, D.S.; Takahashi, H.; Yuste, R. Imaging Voltage in Neurons. *Neuron* **2011**, *69*, 9–21. [[CrossRef](#)] [[PubMed](#)]
7. Djemai, M.; Cupelli, M.; Boutjdir, M.; Chahine, M. Optical Mapping of Cardiomyocytes in Monolayer Derived from Induced Pluripotent Stem Cells. *Cells* **2023**, *12*, 2168. [[CrossRef](#)] [[PubMed](#)]
8. González, J.E.; Tsien, R.Y. Voltage Sensing by Fluorescence Resonance Energy Transfer in Single Cells. *Biophys. J.* **1995**, *69*, 1272–1280. [[CrossRef](#)] [[PubMed](#)]
9. Fumoto, T.; Imato, K.; Ooyama, Y. Elucidation of a Detection Mechanism of a Fluorescent Sensor Based on Photo-Induced Electron Transfer for Water. *New J. Chem.* **2022**, *46*, 21037–21046. [[CrossRef](#)]
10. Hutcheon, B.; Yarom, Y. Resonance, Oscillation and the Intrinsic Frequency Preferences of Neurons. *Trends Neurosci.* **2000**, *23*, 216–222. [[CrossRef](#)] [[PubMed](#)]
11. Scaduto, R.C.; Grotyohann, L.W. Measurement of Mitochondrial Membrane Potential Using Fluorescent Rhodamine Derivatives. *Biophys. J.* **1999**, *76*, 469–477. [[CrossRef](#)]
12. Clapham, D.E. Calcium Signaling. *Cell* **2007**, *131*, 1047–1058. [[CrossRef](#)] [[PubMed](#)]
13. Russell, J.T. Imaging Calcium Signals in Vivo: A Powerful Tool in Physiology and Pharmacology. *Br. J. Pharmacol.* **2011**, *163*, 1605–1625. [[CrossRef](#)]
14. Scherschel, J.A.; Rubart, M. Cardiovascular Imaging Using Two-Photon Microscopy. *Microsc. Microanal.* **2008**, *14*, 492–506. [[CrossRef](#)] [[PubMed](#)]
15. Kee, M.Z.L.; Wuskell, J.P.; Loew, L.M.; Augustine, G.J.; Sekino, Y. Imaging Activity of Neuronal Populations with New Long-Wavelength Voltage-Sensitive Dyes. *Brain Cell Biol.* **2008**, *36*, 157–172. [[CrossRef](#)] [[PubMed](#)]
16. Yan, P.; Acker, C.D.; Zhou, W.-L.; Lee, P.; Bollensdorff, C.; Negrean, A.; Lotti, J.; Sacconi, L.; Antic, S.D.; Kohl, P.; et al. Palette of Fluorinated Voltage-Sensitive Hemicyanine Dyes. *Proc. Natl. Acad. Sci. USA* **2012**, *109*, 20443–20448. [[CrossRef](#)] [[PubMed](#)]
17. Ascoli, G.A.; Bezhanskaya, J.; Tsytsarev, V. Microscopy. In *Encyclopedia of the Neurological Sciences*; Elsevier: Amsterdam, The Netherlands, 2014; pp. 16–20. ISBN 978-0-12-385158-1.
18. Li, J.-H.; Fan, L.-F.; Zhao, D.-J.; Zhou, Q.; Yao, J.-P.; Wang, Z.-Y.; Huang, L. Plant Electrical Signals: A Multidisciplinary Challenge. *J. Plant Physiol.* **2021**, *261*, 153418. [[CrossRef](#)] [[PubMed](#)]
19. Chemla, S.; Chavane, F. Voltage-Sensitive Dye Imaging: Technique Review and Models. *J. Physiol.* **2010**, *104*, 40–50. [[CrossRef](#)] [[PubMed](#)]
20. Miller, E.W. Small Molecule Fluorescent Voltage Indicators for Studying Membrane Potential. *Curr. Opin. Chem. Biol.* **2016**, *33*, 74–80. [[CrossRef](#)]
21. Yu, Q.; Wang, X.; Nie, L. Optical Recording of Brain Functions Based on Voltage-Sensitive Dyes. *Chin. Chem. Lett.* **2021**, *32*, 1879–1887. [[CrossRef](#)]
22. Ebner, T.J.; Chen, G. Use of Voltage-Sensitive Dyes and Optical Recordings in the Central Nervous System. *Prog. Neurobiol.* **1995**, *46*, 463–506. [[CrossRef](#)] [[PubMed](#)]

23. Miller, E.W.; Lin, J.Y.; Frady, E.P.; Steinbach, P.A.; Kristan, W.B.; Tsien, R.Y. Optically Monitoring Voltage in Neurons by Photo-Induced Electron Transfer through Molecular Wires. *Proc. Natl. Acad. Sci.* **2012**, *109*, 2114–2119. [[CrossRef](#)] [[PubMed](#)]
24. Bajar, B.T.; Wang, E.S.; Zhang, S.; Lin, M.Z.; Chu, J. A Guide to Fluorescent Protein FRET Pairs. *Sensors* **2016**, *16*, 1488. [[CrossRef](#)]
25. Broussard, J.A.; Rappaz, B.; Webb, D.J.; Brown, C.M. Fluorescence Resonance Energy Transfer Microscopy as Demonstrated by Measuring the Activation of the Serine/Threonine Kinase Akt. *Nat. Protoc.* **2013**, *8*, 265–281. [[CrossRef](#)]
26. Kiyokawa, E.; Aoki, K.; Nakamura, T.; Matsuda, M. Spatiotemporal Regulation of Small GTPases as Revealed by Probes Based on the Principle of Förster Resonance Energy Transfer (FRET): Implications for Signaling and Pharmacology. *Annu. Rev. Pharmacol. Toxicol.* **2011**, *51*, 337–358. [[CrossRef](#)] [[PubMed](#)]
27. Miyawaki, A. Development of Probes for Cellular Functions Using Fluorescent Proteins and Fluorescence Resonance Energy Transfer. *Annu. Rev. Biochem.* **2011**, *80*, 357–373. [[CrossRef](#)] [[PubMed](#)]
28. Cardullo, R.A. Theoretical Principles and Practical Considerations for Fluorescence Resonance Energy Transfer Microscopy. *Methods Cell Biol.* **2007**, *81*, 479–494. [[CrossRef](#)] [[PubMed](#)]
29. Amero, C.; Schanda, P.; Durá, M.A.; Ayala, I.; Marion, D.; Franzetti, B.; Brutscher, B.; Boisbouvier, J. Fast Two-Dimensional NMR Spectroscopy of High Molecular Weight Protein Assemblies. *J. Am. Chem. Soc.* **2009**, *131*, 3448–3449. [[CrossRef](#)] [[PubMed](#)]
30. Verma, A.K.; Noumani, A.; Yadav, A.K.; Solanki, P.R. FRET Based Biosensor: Principle Applications Recent Advances and Challenges. *Diagnostics* **2023**, *13*, 1375. [[CrossRef](#)]
31. Han, Y.; Fan, X.; Sun, K.; Wang, X.; Wang, Y.; Chen, J.; Zhen, Y.; Zhang, W.; Hui, R. Hypertension Associated Polymorphisms in WNK1/WNK4 Are Not Associated with Hydrochlorothiazide Response. *Clin. Biochem.* **2011**, *44*, 1045–1049. [[CrossRef](#)] [[PubMed](#)]
32. Li, Y.; Sun, C.; Song, P.; Ma, F.; Kungwan, N.; Sun, M. Physical Insight on Mechanism of Photoinduced Charge Transfer in Multipolar Photoactive Molecules. *Sci. Rep.* **2018**, *8*, 10089. [[CrossRef](#)]
33. Wang, S.; Ren, W.X.; Hou, J.-T.; Won, M.; An, J.; Chen, X.; Shu, J.; Kim, J.S. Fluorescence Imaging of Pathophysiological Microenvironments. *Chem. Soc. Rev.* **2021**, *50*, 8887–8902. [[CrossRef](#)]
34. Dey, D.; Sarangi, M.K.; Ray, A.; Bhattacharyya, D.; Maity, D.K. Excited State Hydrogen Bonding Fluorescent Probe: Role of Structure and Environment. *J. Lumin.* **2016**, *173*, 105–112. [[CrossRef](#)]
35. Aigner, D.; Freunberger, S.A.; Wilkening, M.; Saf, R.; Borisov, S.M.; Klimant, I. Enhancing Photoinduced Electron Transfer Efficiency of Fluorescent pH-Probes with Halogenated Phenols. *Anal. Chem.* **2014**, *86*, 9293–9300. [[CrossRef](#)]
36. Bojesomo, R.S.; Saleh, N. Photoinduced Electron Transfer in Encapsulated Heterocycles by Cavitands. *Photochem. Photobiol.* **2022**, *98*, 754–762. [[CrossRef](#)] [[PubMed](#)]
37. Niu, H.; Liu, J.; O'Connor, H.M.; Gunnlaugsson, T.; James, T.D.; Zhang, H. Photoinduced Electron Transfer (PeT) Based Fluorescent Probes for Cellular Imaging and Disease Therapy. *Chem. Soc. Rev.* **2023**, *52*, 2322–2357. [[CrossRef](#)]
38. Nolfi-Donagan, D.; Braganza, A.; Shiva, S. Mitochondrial electron transport chain: Oxidative phosphorylation, oxidant production, and methods of measurement. *Redox Biol.* **2020**, *37*, 101674. [[CrossRef](#)] [[PubMed](#)] [[PubMed Central](#)]
39. Zhang, B.; Pan, C.; Feng, C.; Yan, C.; Yu, Y.; Chen, Z.; Guo, C.; Wang, X. Role of mitochondrial reactive oxygen species in homeostasis regulation. *Redox Rep.* **2022**, *27*, 45–52. [[CrossRef](#)] [[PubMed](#)] [[PubMed Central](#)]
40. Zong, Y.; Li, H.; Liao, P.; Chen, L.; Pan, Y.; Zheng, Y.; Zhang, C.; Liu, D.; Zheng, M.; Gao, J. Mitochondrial dysfunction: Mechanisms and advances in therapy. *Signal Transduct. Target. Ther.* **2024**, *9*, 124. [[CrossRef](#)] [[PubMed](#)]
41. Zorova, L.D.; Popkov, V.A.; Plotnikov, E.Y.; Silachev, D.N.; Pevzner, I.B.; Jankauskas, S.S.; Babenko, V.A.; Zorov, S.D.; Balakireva, A.V.; Juhaszova, M.; et al. Mitochondrial membrane potential. *Anal. Biochem.* **2018**, *552*, 50–59. [[CrossRef](#)] [[PubMed](#)] [[PubMed Central](#)]
42. Shivling Mali, A.; Honc, O.; Hejnova, L.; Novotny, J. Opioids Alleviate Oxidative Stress via the Nrf2/HO-1 Pathway in LPS-Stimulated Microglia. *Int. J. Mol. Sci.* **2023**, *24*, 11089. [[CrossRef](#)]
43. Nunnari, J.; Suomalainen, A. Mitochondria: In Sickness and in Health. *Cell* **2012**, *148*, 1145–1159. [[CrossRef](#)] [[PubMed](#)]
44. De Souza Breda, C.N.; Davanzo, G.G.; Basso, P.J.; Câmara, N.O.S.; Moraes-Vieira, P.M.M. Mitochondria as central hub of the immune system. *Redox Biol.* **2019**, *26*, 101255. [[CrossRef](#)]
45. Klier, P.E.Z.; Roo, R.; Miller, E.W. Fluorescent Indicators for Imaging Membrane Potential of Organelles. *Curr. Opin. Chem. Biol.* **2022**, *71*, 102203. [[CrossRef](#)] [[PubMed](#)]
46. Carlson, G.C.; Coulter, D.A. In Vitro Functional Imaging in Brain Slices Using Fast Voltage-Sensitive Dye Imaging Combined with Whole-Cell Patch Recording. *Nat. Protoc.* **2008**, *3*, 249–255. [[CrossRef](#)] [[PubMed](#)]
47. Pak, R.W.; Kang, J.; Boctor, E.; Kang, J.U. Optimization of Near-Infrared Fluorescence Voltage-Sensitive Dye Imaging for Neuronal Activity Monitoring in the Rodent Brain. *Front. Neurosci.* **2021**, *15*, 742405. [[CrossRef](#)]
48. Yan, P.; Acker, C.D.; Biasci, V.; Judge, G.; Monroe, A.; Sacconi, L.; Loew, L.M. Near-Infrared Voltage-Sensitive Dyes Based on Chromene Donor. *Proc. Natl. Acad. Sci. USA* **2023**, *120*, e2305093120. [[CrossRef](#)]
49. Salama, G.; Choi, B.-R.; Azour, G.; Lavasani, M.; Tumbey, V.; Salzberg, B.M.; Patrick, M.J.; Ernst, L.A.; Waggoner, A.S. Properties of New, Long-Wavelength, Voltage-Sensitive Dyes in the Heart. *J. Membr. Biol.* **2005**, *208*, 125–140. [[CrossRef](#)]
50. Song, G.; He, H.; Chen, W.; Lv, Y.; Chu, P.K.; Wang, H.; Li, P. Reversibly Migratable Fluorescent Probe for Precise and Dynamic Evaluation of Cell Mitochondrial Membrane Potentials. *Biosensors* **2022**, *12*, 798. [[CrossRef](#)] [[PubMed](#)]
51. Hernández-Juárez, C.; Calahorra, M.; Peña, A.; Jiménez-Sánchez, A. Fluorescent Probe as Dual-Organelle Localizer Through Differential Proton Gradients Between Lipid Droplets and Mitochondria. *Anal. Chem.* **2024**, *96*, 9262–9269. [[CrossRef](#)] [[PubMed](#)]
52. Sivandzade, F.; Bhalerao, A.; Cucullo, L. Analysis of the Mitochondrial Membrane Potential Using the Cationic JC-1 Dye as a Sensitive Fluorescent Probe. *Bio-Protocol* **2019**, *9*, e3128. [[CrossRef](#)]

53. Perry, S.W.; Norman, J.P.; Barbieri, J.; Brown, E.B.; Gelbard, H.A. Mitochondrial Membrane Potential Probes and the Proton Gradient: A Practical Usage Guide. *BioTechniques* **2011**, *50*, 98–115. [[CrossRef](#)]
54. Baracca, A.; Sgarbi, G.; Solaini, G.; Lenaz, G. Rhodamine 123 as a Probe of Mitochondrial Membrane Potential: Evaluation of Proton Flux through F(0) during ATP Synthesis. *Biochim. Biophys. Acta* **2003**, *1606*, 137–146. [[CrossRef](#)]
55. Manno, C.; Figueroa, L.; Fitts, R.; Ríos, E. Confocal Imaging of Transmembrane Voltage by SEER of Di-8-ANEPPS. *J. Gen. Physiol.* **2013**, *141*, 371–387. [[CrossRef](#)]
56. Youngworth, R.; Roux, B. Simulating the Voltage-Dependent Fluorescence of Di-8-ANEPPS in a Lipid Membrane. *J. Phys. Chem. Lett.* **2023**, *14*, 8268–8276. [[CrossRef](#)]
57. Ernst, P.; Kim, S.; Yang, Z.; Liu, X.M.; Zhou, L. Characterization of the Far-Red Fluorescent Probe MitoView 633 for Dynamic Mitochondrial Membrane Potential Measurement. *Front. Physiol.* **2023**, *14*, 1257739. [[CrossRef](#)] [[PubMed](#)]
58. Creed, S.; McKenzie, M. Measurement of Mitochondrial Membrane Potential with the Fluorescent Dye Tetramethylrhodamine Methyl Ester (TMRM). *Methods Mol. Biol.* **2019**, *1928*, 69–76. [[CrossRef](#)]
59. Kholmukhamedov, A.; Schwartz, J.M.; Lemasters, J.J. Isolated Mitochondria Infusion Mitigates Ischemia-Reperfusion Injury of the Liver in Rats: Mitotracker Probes and Mitochondrial Membrane Potential. *Shock* **2013**, *39*, 543. [[CrossRef](#)] [[PubMed](#)]
60. Buravkov, S.V.; Pogodina, M.V.; Buravkova, L.B. Comparison of Mitochondrial Fluorescent Dyes in Stromal Cells. *Bull. Exp. Biol. Med.* **2014**, *157*, 654–658. [[CrossRef](#)]
61. Neikirk, K.; Marshall, A.G.; Kula, B.; Smith, N.; LeBlanc, S.; Hinton, A. MitoTracker: A useful tool in need of better alternatives. *Eur. J. Cell Biol.* **2023**, *102*, 151371. [[CrossRef](#)] [[PubMed](#)]
62. Wang, Q.; Zou, M.-H. Measurement of Reactive Oxygen Species (ROS) and Mitochondrial ROS in AMPK Knockout Mice Blood Vessels. *Methods Mol. Biol.* **2018**, *1732*, 507–517. [[CrossRef](#)] [[PubMed](#)]
63. Roelofs, B.A.; Ge, S.X.; Studlack, P.E.; Polster, B.M. Low Micromolar Concentrations of the Superoxide Probe MitoSOX Un-couple Neural Mitochondria and Inhibit Complex IV. *Free Radic. Biol. Med.* **2015**, *86*, 250–258. [[CrossRef](#)]
64. Krumshabel, G.; Eigentler, A.; Fasching, M.; Gnaiger, E. Use of Safranin for the Assessment of Mitochondrial Membrane Potential by High-Resolution Respirometry and Fluorometry. *Methods Enzymol.* **2014**, *542*, 163–181. [[CrossRef](#)]
65. Chowdhury, S.R.; Djordjevic, J.; Albensi, B.C.; Fernyhough, P. Simultaneous Evaluation of Substrate-Dependent Oxygen Consumption Rates and Mitochondrial Membrane Potential by TMRM and Safranin in Cortical Mitochondria. *Biosci. Rep.* **2015**, *36*, e00286. [[CrossRef](#)]
66. Younes, N.; Alsaah, B.S.; Al-Mesaifri, A.J.; Da'as, S.I.; Pintus, G.; Majdalawieh, A.F.; Nasrallah, G.K. JC-10 Probe as a Novel Method for Analyzing the Mitochondrial Membrane Potential and Cell Stress in Whole Zebrafish Embryos. *Toxicol. Res.* **2022**, *11*, 77–87. [[CrossRef](#)] [[PubMed](#)]
67. Sakamuru, S.; Attene-Ramos, M.S.; Xia, M. Mitochondrial Membrane Potential Assay. *Methods Mol. Biol.* **2016**, *1473*, 17–22. [[CrossRef](#)] [[PubMed](#)]
68. Ramadass, R.; Bereiter-Hahn, J. How DASPMI Reveals Mitochondrial Membrane Potential: Fluorescence Decay Kinetics and Steady-State Anisotropy in Living Cells. *Biophys. J.* **2008**, *95*, 4068–4076. [[CrossRef](#)]
69. McCracken, D.J.; Lovasik, B.P.; McCracken, C.E.; Caplan, J.M.; Turan, N.; Nogueira, R.G.; Cawley, C.M.; Dion, J.E.; Tamargo, R.J.; Barrow, D.L.; et al. Resolution of Oculomotor Nerve Palsy Secondary to Posterior Communicating Artery Aneurysms: Comparison of Clipping and Coiling. *Neurosurgery* **2015**, *77*, 931–939, discussion 939. [[CrossRef](#)]
70. Swidah, R.; Ogunlabi, O.; Grant, C.M.; Ashe, M.P. N-Butanol Production in *S. Cerevisiae*: Co-Ordinate Use of Endogenous and Exogenous Pathways. *Appl. Microbiol. Biotechnol.* **2018**, *102*, 9857–9866. [[CrossRef](#)]
71. Oh, J.; Lee, C.; Kaang, B.-K. Imaging and Analysis of Genetically Encoded Calcium Indicators Linking Neural Circuits and Behaviors. *Korean J. Physiol. Pharmacol.* **2019**, *23*, 237–249. [[CrossRef](#)] [[PubMed](#)]
72. Aseyev, N.; Ivanova, V.; Balaban, P.; Nikitin, E. Current Practice in Using Voltage Imaging to Record Fast Neuronal Activity: Successful Examples from Invertebrate to Mammalian Studies. *Biosensors* **2023**, *13*, 648. [[CrossRef](#)]
73. Grienberger, C.; Chen, X.; Konnerth, A. Dendritic Function In Vivo. *Trends Neurosci.* **2015**, *38*, 45–54. [[CrossRef](#)]
74. Antic, S.D.; Empson, R.M.; Knöpfel, T. Voltage imaging to understand connections and functions of neuronal circuits. *J. Neurophysiol.* **2016**, *116*, 135–152. [[CrossRef](#)] [[PubMed](#)]
75. Hochbaum, D.R.; Zhao, Y.; Farhi, S.L.; Klapoetke, N.; Werley, C.A.; Kapoor, V.; Zou, P.; Kralj, J.M.; Maclaurin, D.; Smedemark-Margulies, N.; et al. All-Optical Electrophysiology in Mammalian Neurons Using Engineered Microbial Rhodopsins. *Nat. Methods* **2014**, *11*, 825–833. [[CrossRef](#)]
76. Piatkevich, K.D.; Jung, E.E.; Straub, C.; Linghu, C.; Park, D.; Suk, H.-J.; Hochbaum, D.R.; Goodwin, D.; Pnevmatikakis, E.; Pak, N.; et al. A Robotic Multidimensional Directed Evolution Approach Applied to Fluorescent Voltage Reporters. *Nat. Chem. Biol.* **2018**, *14*, 352–360. [[CrossRef](#)]
77. Fisher, J.A.N.; Salzberg, B.M. Two-Photon Excitation of Fluorescent Voltage-Sensitive Dyes: Monitoring Membrane Potential in the Infrared. *Adv. Exp. Med. Biol.* **2015**, *859*, 427–453. [[CrossRef](#)] [[PubMed](#)]
78. Karlstad, J.; Sun, Y.; Singh, B.B. Ca²⁺ Signaling: An Outlook on the Characterization of Ca(2+) Channels and Their Importance in Cellular Functions. *Adv. Exp. Med. Biol.* **2012**, *740*, 143–157. [[CrossRef](#)]
79. Santofimia-Castaño, P.; Salido, G.M.; Gonzalez, A. Interferences of Resveratrol with Fura-2-Derived Fluorescence in Intracellular Free-Ca²⁺ Concentration Determinations. *Cytotechnology* **2016**, *68*, 1369–1380. [[CrossRef](#)] [[PubMed](#)]

80. Tanaka, M.; Matsui, T. Methodologies for Investigating the Vasorelaxation Action of Peptides. In *Biologically Active Peptides*; Elsevier: Amsterdam, The Netherlands, 2021; pp. 255–274. ISBN 978-0-12-821389-6.
81. Li, E.S.; Saha, M.S. Optimizing Calcium Detection Methods in Animal Systems: A Sandbox for Synthetic Biology. *Biomolecules* **2021**, *11*, 343. [[CrossRef](#)] [[PubMed](#)] [[PubMed Central](#)]
82. Schneidereit, D.; Vass, H.; Reischl, B.; Allen, R.J.; Friedrich, O. Calcium Sensitive Fluorescent Dyes Fluo-4 and Fura Red under Pressure: Behaviour of Fluorescence and Buffer Properties under Hydrostatic Pressures up to 200 MPa. *PLoS ONE* **2016**, *11*, e0164509. [[CrossRef](#)]
83. Gee, K.R.; Brown, K.A.; Chen, W.-N.U.; Bishop-Stewart, J.; Gray, D.; Johnson, I. Chemical and Physiological Characterization of Fluo-4 Ca²⁺-Indicator Dyes. *Cell Calcium* **2000**, *27*, 97–106. [[CrossRef](#)]
84. Pydi, S.P.; Bhullar, R.P.; Chelikani, P. Constitutive activity of bitter taste receptors (T2Rs). In *Advances in Pharmacology*; Elsevier: Amsterdam, The Netherlands, 2014; pp. 303–326. [[CrossRef](#)]
85. Shen, Y.; Dana, H.; Abdelfattah, A.S.; Patel, R.; Shea, J.; Molina, R.S.; Rawal, B.; Rancic, V.; Chang, Y.-F.; Wu, L.; et al. A Genetically Encoded Ca²⁺ Indicator Based on Circularly Permutated Sea Anemone Red Fluorescent Protein eqFP578. *BMC Biol.* **2018**, *16*, 9. [[CrossRef](#)] [[PubMed](#)]
86. Berlin, S.; Carroll, E.C.; Newman, Z.L.; Okada, H.O.; Quinn, C.M.; Kallman, B.; Rockwell, N.C.; Martin, S.S.; Lagarias, J.C.; Isacoff, E.Y. Photoactivatable Genetically Encoded Calcium Indicators for Targeted Neuronal Imaging. *Nat. Methods* **2015**, *12*, 852–858. [[CrossRef](#)] [[PubMed](#)]
87. Cho, J.; Swanson, C.J.; Chen, J.; Li, A.; Lippert, L.G.; Boye, S.E.; Rose, K.; Sivaramakrishnan, S.; Chuong, C.; Chow, R.H. The GCaMP-R Family of Genetically Encoded Ratiometric Calcium Indicators. *ACS Chem. Biol.* **2017**, *12*, 1066–1074. [[CrossRef](#)] [[PubMed](#)]
88. Drummond, R.M.; Mix, T.C.; Tuft, R.A.; Walsh, J.V.; Fay, F.S. Mitochondrial Ca²⁺ Homeostasis during Ca²⁺ Influx and Ca²⁺ Release in Gastric Myocytes from Bufo Marinus. *J. Physiol.* **2000**, *522 Pt 3*, 375–390. [[CrossRef](#)] [[PubMed](#)]
89. Gryniewicz, G.; Poenie, M.; Tsien, R.Y. A new generation of Ca²⁺ indicators with greatly improved fluorescence properties. *J. Biol. Chem.* **1985**, *260*, 3440–3450. [[CrossRef](#)] [[PubMed](#)]
90. Tischbirek, C.; Birkner, A.; Jia, H.; Sakmann, B.; Konnerth, A. Deep Two-Photon Brain Imaging with a Red-Shifted Fluorometric Ca²⁺ Indicator. *Proc. Natl. Acad. Sci. USA* **2015**, *112*, 11377–11382. [[CrossRef](#)]
91. Lock, J.T.; Parker, I.; Smith, I.F. A Comparison of Fluorescent Ca²⁺ Indicators for Imaging Local Ca²⁺ Signals in Cultured Cells. *Cell Calcium* **2015**, *58*, 638–648. [[CrossRef](#)] [[PubMed](#)]
92. Tada, M.; Takeuchi, A.; Hashizume, M.; Kitamura, K.; Kano, M. A Highly Sensitive Fluorescent Indicator Dye for Calcium Imaging of Neural Activity in Vitro and in Vivo. *Eur. J. Neurosci.* **2014**, *39*, 1720–1728. [[CrossRef](#)] [[PubMed](#)]
93. Bannwarth, M.; Correa, I.R.; Sztretye, M.; Pouvreau, S.; Fellay, C.; Aebischer, A.; Royer, L.; Rois, E.; Johnsson, K. Indo-1 Derivatives for Local Calcium Sensing. *ACS Chem. Biol.* **2009**, *4*, 179–190. [[CrossRef](#)]
94. Ryan, J.; Urayama, P. Characterizing the dual-wavelength dye indo-1 for calcium-ion sensing under pressure. *Anal. Methods* **2011**, *4*, 80–84. [[CrossRef](#)]
95. Salerno, S.; Garten, K.; Smith, G.L.; Stølen, T.; Kelly, A. Two-Photon Excitation of FluoVolt Allows Improved Interrogation of Transmural Electrophysiological Function in the Intact Mouse Heart. *Prog. Biophys. Mol. Biol.* **2020**, *154*, 11–20. [[CrossRef](#)] [[PubMed](#)]
96. Kulkarni, R.U.; Vandenberghe, M.; Thunemann, M.; James, F.; Andreassen, O.A.; Djurovic, S.; Devor, A.; Miller, E.W. In Vivo Two-Photon Voltage Imaging with Sulfonated Rhodamine Dyes. *ACS Cent. Sci.* **2018**, *4*, 1371–1378. [[CrossRef](#)] [[PubMed](#)]
97. Benninger, R.K.P.; Piston, D.W. Two-Photon Excitation Microscopy for the Study of Living Cells and Tissues. *Curr. Protoc. Cell Biol.* **2013**, *59*, 4.11.1–4.11.24. [[CrossRef](#)]
98. Homma, R.; Baker, B.J.; Jin, L.; Garaschuk, O.; Konnerth, A.; Cohen, L.B.; Zecevic, D. Wide-Field and Two-Photon Imaging of Brain Activity with Voltage- and Calcium-Sensitive Dyes. *Philos. Trans. R. Soc. Lond. B Biol. Sci.* **2009**, *364*, 2453–2467. [[CrossRef](#)]
99. Chaigneau, E.; Wright, A.J.; Poland, S.P.; Girkin, J.M.; Silver, R.A. Impact of Wavefront Distortion and Scattering on 2-Photon Microscopy in Mammalian Brain Tissue. *Opt. Express* **2011**, *19*, 22755–22774. [[CrossRef](#)]
100. Niesner, R.; Andresen, V.; Neumann, J.; Spiecker, H.; Gunzer, M. The Power of Single and Multibeam Two-Photon Microscopy for High-Resolution and High-Speed Deep Tissue and Intravital Imaging. *Biophys. J.* **2007**, *93*, 2519–2529. [[CrossRef](#)]
101. Roome, C.J.; Kuhn, B. Dendritic Coincidence Detection in Purkinje Neurons of Awake Mice. *Elife* **2020**, *9*, e59619. [[CrossRef](#)] [[PubMed](#)]
102. Malvaut, S.; Constantinescu, V.-S.; Dehez, H.; Doric, S.; Saghatelian, A. Deciphering Brain Function by Miniaturized Fluorescence Microscopy in Freely Behaving Animals. *Front. Neurosci.* **2020**, *14*, 819. [[CrossRef](#)] [[PubMed](#)]
103. Kwon, J.; Elgawish, M.S.; Shim, S.-H. Bleaching-Resistant Super-Resolution Fluorescence Microscopy. *Adv. Sci.* **2022**, *9*, e2101817. [[CrossRef](#)]
104. Patterson, G.H.; Piston, D.W. Photobleaching in Two-Photon Excitation Microscopy. *Biophys. J.* **2000**, *78*, 2159–2162. [[CrossRef](#)]
105. Dempsey, G.T.; Vaughan, J.C.; Chen, K.H.; Bates, M.; Zhuang, X. Evaluation of Fluorophores for Optimal Performance in Localization-Based Super-Resolution Imaging. *Nat. Methods* **2011**, *8*, 1027–1036. [[CrossRef](#)] [[PubMed](#)]
106. Nolting, D.D.; Gore, J.C.; Pham, W. NEAR-INFRARED DYES: Probe Development and Applications in Optical Molecular Imaging. *Curr. Org. Synth.* **2011**, *8*, 521–534. [[CrossRef](#)] [[PubMed](#)]

107. Davis, A.S.; Richter, A.; Becker, S.; Moyer, J.E.; Sandouk, A.; Skinner, J.; Taubenberger, J.K. Characterizing and Diminishing Autofluorescence in Formalin-Fixed Paraffin-Embedded Human Respiratory Tissue. *J. Histochem. Cytochem.* **2014**, *62*, 405–423. [[CrossRef](#)]
108. Jin, L.; Han, Z.; Platisa, J.; Woollorton, J.R.A.; Cohen, L.B.; Pieribone, V.A. Single Action Potentials and Subthreshold Electrical Events Imaged in Neurons with a Fluorescent Protein Voltage Probe. *Neuron* **2012**, *75*, 779–785. [[CrossRef](#)]
109. Gong, Y.; Huang, C.; Li, J.Z.; Grewe, B.F.; Zhang, Y.; Eismann, S.; Schnitzer, M.J. High-Speed Recording of Neural Spikes in Awake Mice and Flies with a Fluorescent Voltage Sensor. *Science* **2015**, *350*, 1361–1366. [[CrossRef](#)]
110. Abdelfattah, A.S.; Kawashima, T.; Singh, A.; Novak, O.; Liu, H.; Shuai, Y.; Huang, Y.-C.; Campagnola, L.; Seeman, S.C.; Yu, J.; et al. Bright and Photostable Chemigenetic Indicators for Extended in Vivo Voltage Imaging. *Science* **2019**, *365*, 699–704. [[CrossRef](#)] [[PubMed](#)]
111. Kannan, M.; Vasan, G.; Haziza, S.; Huang, C.; Chrapkiewicz, R.; Luo, J.; Cardin, J.A.; Schnitzer, M.J.; Pieribone, V.A. Dual-Polarity Voltage Imaging of the Concurrent Dynamics of Multiple Neuron Types. *Science* **2022**, *378*, eabm8797. [[CrossRef](#)] [[PubMed](#)]
112. Chen, G.; Cao, Y.; Tang, Y.; Yang, X.; Liu, Y.; Huang, D.; Zhang, Y.; Li, C.; Wang, Q. Advanced Near-Infrared Light for Monitoring and Modulating the Spatiotemporal Dynamics of Cell Functions in Living Systems. *Adv. Sci.* **2020**, *7*, 1903783. [[CrossRef](#)] [[PubMed](#)]
113. Ronzhina, M.; Stracina, T.; Lacinova, L.; Ondacova, K.; Pavlovicova, M.; Marsanova, L.; Smisek, R.; Janousek, O.; Fialova, K.; Kolarova, J.; et al. Di-4-ANEPPS Modulates Electrical Activity and Progress of Myocardial Ischemia in Rabbit Isolated Heart. *Front. Physiol.* **2021**, *12*, 667065. [[CrossRef](#)]
114. Herron, T.J.; Lee, P.; Jalife, J. Optical Imaging of Voltage and Calcium in Cardiac Cells & Tissues. *Circ. Res.* **2012**, *110*, 609–623. [[CrossRef](#)]
115. Grimm, J.B.; Tkachuk, A.N.; Patel, R.; Hennigan, S.T.; Gutu, A.; Dong, P.; Gandin, V.; Osowski, A.M.; Holland, K.L.; Liu, Z.J.; et al. Optimized Red-Absorbing Dyes for Imaging and Sensing. *J. Am. Chem. Soc.* **2023**, *145*, 23000–23013. [[CrossRef](#)] [[PubMed](#)]
116. Hübener, G.; Lambacher, A.; Fromherz, P. Anellated Hemicyanine Dyes with Large Symmetrical Solvatochromism of Absorption and Fluorescence. *J. Phys. Chem. B* **2003**, *107*, 7896–7902. [[CrossRef](#)]
117. Hassner, A.; Birnbaum, D.; Loew, L.M. Charge-Shift Probes of Membrane Potential. *Synthesis. J. Org. Chem.* **1984**, *49*, 2546–2551. [[CrossRef](#)]
118. Röcker, C.; Heilemann, A.; Fromherz, P. Time-Resolved Fluorescence of a Hemicyanine Dye: Dynamics of Rotamerism and Resolution. *J. Phys. Chem.* **1996**, *100*, 12172–12177. [[CrossRef](#)]
119. Kirmse, W.; Kund, K. Intramolecular Generation of Oxonium Ylides from Functionalized Arylcarbenes. *J. Am. Chem. Soc.* **1989**, *111*, 1465–1473. [[CrossRef](#)]
120. Kumari, K.; Raghuvanshi, D.S.; Singh, K.N. An Efficient Synthesis of 2H-Chromen-3-Yl Derivatives via CuI/(NH₄)₂HPO₄ Catalyzed Reaction of O-Propargyl Salicylaldehydes with Active Methylene Compounds. *Tetrahedron* **2013**, *69*, 82–88. [[CrossRef](#)]
121. Fromherz, P.; Hübener, G.; Kuhn, B.; Hinner, M.J. ANNINE-6plus, a Voltage-Sensitive Dye with Good Solubility, Strong Membrane Binding and High Sensitivity. *Eur. Biophys. J.* **2008**, *37*, 509–514. [[CrossRef](#)] [[PubMed](#)]
122. Raliski, B.K.; Kirk, M.J.; Miller, E.W. Imaging Spontaneous Neuronal Activity with Voltage-Sensitive Dyes. *Curr. Protoc.* **2021**, *1*, e48. [[CrossRef](#)]
123. Bando, Y.; Grimm, C.; Cornejo, V.H.; Yuste, R. Genetic Voltage Indicators. *BMC Biol.* **2019**, *17*, 71. [[CrossRef](#)] [[PubMed](#)]
124. Marchal, G.A.; Biasci, V.; Yan, P.; Palandri, C.; Campione, M.; Cerbai, E.; Loew, L.M.; Sacconi, L. Recent Advances and Current Limitations of Available Technology to Optically Manipulate and Observe Cardiac Electrophysiology. *Pflugers Arch. Eur. J. Physiol.* **2023**, *475*, 1357–1366. [[CrossRef](#)] [[PubMed](#)]
125. Hoffmann, R.; Stellbrink, E.; Schröder, J.; Grawe, A.; Vogel, G.; Blindt, R.; Kelm, M.; Radke, P.W. Impact of the Metabolic Syndrome on Angiographic and Clinical Events after Coronary Intervention Using Bare-Metal or Sirolimus-Eluting Stents. *Am. J. Cardiol.* **2007**, *100*, 1347–1352. [[CrossRef](#)] [[PubMed](#)]
126. Bernstein, C.N.; Wajda, A.; Blanchard, J.F. The Incidence of Arterial Thromboembolic Diseases in Inflammatory Bowel Disease: A Population-Based Study. *Clin. Gastroenterol. Hepatol.* **2008**, *6*, 41–45. [[CrossRef](#)]
127. Chien, M.-P.; Brinks, D.; Testa-Silva, G.; Tian, H.; Phil Brooks, F.; Adam, Y.; Bloxham, B.; Gmeiner, B.; Kheifets, S.; Cohen, A.E. Photoactivated Voltage Imaging in Tissue with an Archaelhodopsin-Derived Reporter. *Sci. Adv.* **2021**, *7*, eabe3216. [[CrossRef](#)] [[PubMed](#)]
128. Lin, J.Y.; Knutsen, P.M.; Muller, A.; Kleinfeld, D.; Tsien, R.Y. ReaChR: A Red-Shifted Variant of Channelrhodopsin Enables Deep Transcranial Optogenetic Excitation. *Nat. Neurosci.* **2013**, *16*, 1499–1508. [[CrossRef](#)]
129. Xu, Y.; Zou, P.; Cohen, A.E. Voltage Imaging with Genetically Encoded Indicators. *Curr. Opin. Chem. Biol.* **2017**, *39*, 1–10. [[CrossRef](#)] [[PubMed](#)]
130. Chabala, L.I. Functional and structural transformation of chromosomes of various proliferating hematopoietic cells of the bone marrow in albino rats. *Kosm. Biol. Aviakosm. Med.* **1986**, *20*, 78–80.
131. Attin, M.; Clusin, W.T. Basic Concepts of Optical Mapping Techniques in Cardiac Electrophysiology. *Biol. Res. Nurs.* **2009**, *11*, 195–207. [[CrossRef](#)] [[PubMed](#)]
132. Baker, B.J.; Mutoh, H. Dynamic Imaging of Neural Activity Using Genetically Encoded Voltage Indicators. *Front. Cell. Neurosci.* **2015**, *9*, 311. [[CrossRef](#)]

133. Loew, L.M.; Simpson, L.L. Charge-Shift Probes of Membrane Potential: The Molecular Basis of Voltage-Sensitive Fluorescence. *Biophys. J.* **1981**, *34*, 353–365. [[CrossRef](#)] [[PubMed](#)]
134. Ghoroghchian, P.P.; Therien, M.J.; Hammer, D.A. In vivo fluorescence imaging: A personal perspective. *Wiley Interdiscip. Rev. Nanomed. Nanobiotechnol.* **2009**, *1*, 156–167. [[CrossRef](#)] [[PubMed](#)]
135. Grenier, V.; Daws, B.R.; Liu, P.; Miller, E.W. Spying on Neuronal Membrane Potential with Genetically Targetable Voltage Indicators. *J. Am. Chem. Soc.* **2019**, *141*, 1349–1358. [[CrossRef](#)]
136. Loew, L.M. Design and Use of Organic Voltage Sensitive Dyes. *Adv. Exp. Med. Biol.* **2015**, *859*, 27–53. [[CrossRef](#)] [[PubMed](#)]
137. Liu, W.Y.; Li, H.Y.; Lv, H.S.; Zhao, B.X.; Miao, J.Y. A rhodamine chromene-based turn-on fluorescence probe for selectively imaging Cu²⁺ in living cell. *Spectrochim. Acta A Mol. Biomol. Spectrosc.* **2012**, *95*, 658–663. [[CrossRef](#)] [[PubMed](#)]
138. Kuhn, B.; Roome, C.J. Primer to Voltage Imaging With ANNINE Dyes and Two-Photon Microscopy. *Front. Cell. Neurosci.* **2019**, *13*, 321. [[CrossRef](#)] [[PubMed](#)]

Disclaimer/Publisher’s Note: The statements, opinions and data contained in all publications are solely those of the individual author(s) and contributor(s) and not of MDPI and/or the editor(s). MDPI and/or the editor(s) disclaim responsibility for any injury to people or property resulting from any ideas, methods, instructions or products referred to in the content.